

A novel CD71 Centyrin:Gys1 siRNA conjugate reduces glycogen synthesis and glycogen levels in a mouse model of Pompe disease

Bryce D. Holt,¹ Samuel J. Elliott,¹ Rebecca Meyer,² Daniela Reyes,² Karyn O'Neil,² Zhanna Druzina,² Swapnil Kulkarni,² Beth L. Thurberg,³ Steven G. Nadler,² and Bartholomew A. Pederson^{4,5}

¹Department of Biology, Ball State University, Muncie, IN 47306, USA; ²Aro Biotherapeutics, Philadelphia, PA 19106, USA; ³Beth Thurberg Orphan Science Consulting LLC, Newton, MA 02458, USA; ⁴Center for Medical Education, Ball State University, Muncie, IN 47306, USA; ⁵Department of Biochemistry and Molecular Biology, Indiana University School of Medicine-Muncie, Muncie, IN 47303, USA

Pompe disease is caused by acid alpha-glucosidase (GAA) deficiency, resulting in lysosomal glycogen accumulation. This disease is characterized by progressive skeletal muscle weakness, respiratory distress, and in the infantile-onset form, cardiomyopathy. The only approved treatment is enzyme replacement therapy (ERT) with human recombinant GAA. While ERT therapy extends life span, residual symptoms remain, with poor muscle uptake and immunogenicity limiting efficacy. We examined a novel Centyrin protein—short interfering ribonucleic acid (siRNA) conjugate targeting CD71 (transferrin receptor type 1, TfR1) and GYS1, a key enzyme involved in glycogen synthesis. Unlike existing ERTs designed to degrade aberrant glycogen deposits observed in Pompe patients, the CD71 Centyrin:Gys1 siRNA is designed to restore glycogen balance by inhibiting glycogen synthesis. To this end, we administered the CD71 Centyrin:Gys1 siRNA conjugate to the $\epsilon^{neo}/\epsilon^{neo}$ Pompe mouse model. Once bound to TfR1, siRNA-conjugated Centyrin is internalized into cells to facilitate gene knockdown. We found that treatment with this conjugate significantly reduced GYS1 protein expression, glycogen synthase enzymatic activity, and glycogen levels in muscle. In addition, impaired treadmill exercise performance of male Pompe mice was improved. These data suggest that Centyrin-mediated delivery of Gys1 siRNA may be an effective next generation therapy for late-onset Pompe disease or, in combination with ERT, for infantile-onset Pompe disease.

INTRODUCTION

Pompe disease (PD), type II glycogen storage disease, is caused by the nearly 600 currently known mutations of the *Gaa* gene, resulting in deficient or missing acid alpha-glucosidase (GAA). GAA is present in lysosomes and catalyzes hydrolysis of alpha-1,4-glycosidic bonds in glycogen releasing glucose. This process, termed glycophagy, involves membrane engulfment of cytosolic glycogen into an autophagosome that fuses with lysosomes to form autophagolysosomes.¹ In PD, this mechanism for degrading glycogen is compromised, due to *Gaa* insufficiency, resulting in dramatic lysosomal glycogen overaccu-

mulation in multiple tissues. Phenotypically, PD shows a wide variety of clinical symptoms that vary based on age of onset. PD is largely split into two broad categories, late-onset (LOPD) and infantile-onset (IOPD), that show symptoms after and before 12 months of age, respectively. A majority of LOPD patients show hallmark symptoms of proximal limb-girdle muscle myopathy. The progression of disease symptoms is relatively slow but will ultimately lead to intense muscle weakness and eventual wasting. Patients in later stages of the disease will become wheelchair dependent and respiratory failure is common due to the involvement of the diaphragm. IOPD is characterized by comparatively more aggressive symptoms, such as progressive hypertrophic cardiomyopathy and left ventricular outflow obstruction. Symptoms of muscle weakness, respiratory distress, and eventual loss of independent ventilation, and feeding are also common. Motor development is significantly delayed, and major developmental milestones, such as the ability to roll over, sit, or stand, are often not achieved. Without treatment, infants with this variation of the disease rarely survive beyond 1 year of age due to cardiac and respiratory complications resulting from severe muscle weakness.^{2,3}

Currently the only approved form of treatment for PD is enzyme replacement therapy (ERT) with human recombinant acid alpha-glucosidase (rhGAA) which is typically administered biweekly over several hours. The first clinical trials of ERT were conducted in IOPD patients and showed relative success.⁴ In a study of 18 PD patients younger than 6 months of age, all lived to age 18 months. However, a 3-year extension to the trial saw the survival rate and independent ventilation rate drop to 67.5% and 50% respectively. In another study of 20 infantile-onset diseased patients, the survival rate was lower at 65%, with 30% of total patients becoming ventilated.⁵ There is poor efficacy of this treatment in skeletal muscle of a subset of IOPD patients that make no GAA (CRIM-negative patients) and generate antibodies to the ERT enzyme.

Received 19 June 2024; accepted 22 November 2024;
<https://doi.org/10.1016/j.ymthe.2024.11.033>

Correspondence: Bartholomew A. Pederson, Center for Medical Education, Ball State University, Muncie, IN 47306, USA.

E-mail: bapederson@bsu.edu



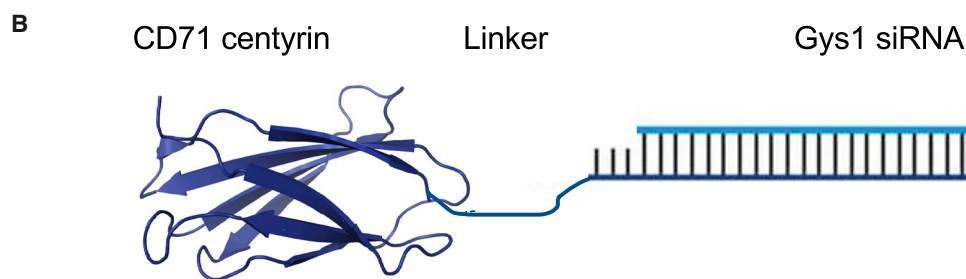
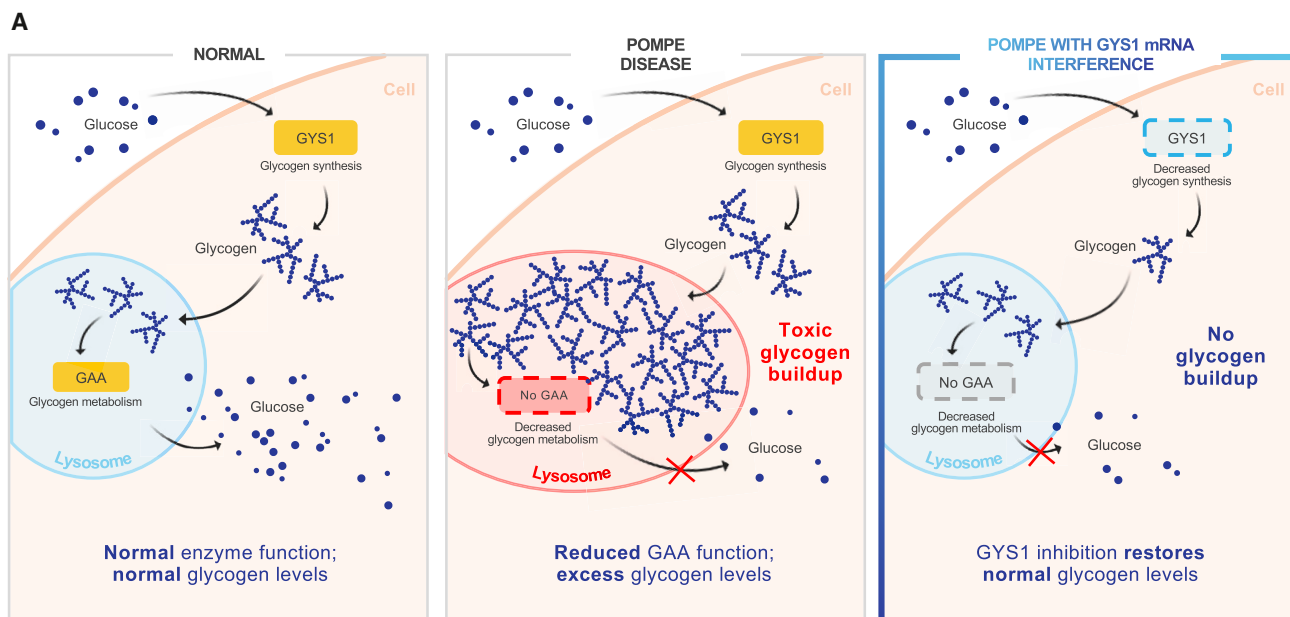


Figure 1. Model of CD71 Centyrin-Gys1 siRNA treatment strategy

(A) Normally (left panel), glycogen is synthesized in the cytosol and a portion is taken up into lysosomes where it is degraded to glucose by GAA. In PD (middle panel), glycogen synthesis remains intact and glycogen accumulates in lysosomes due to deficient GAA activity. CD71 Centyrin:Gys1 siRNA decreases the amount of GYS1 protein expression, leading to reduced glycogen synthesis in PD (right panel). The impact of this treatment on lysosomal glycogen accumulation will be dependent on the amount of cellular GYS1 and GAA activity. (B) CD71 Centyrin conjugated to Gys1 siRNA binds to transferrin type 1 receptor leading to internalization and expected inhibition of Gys1 expression.

This has prompted the use of immunomodulators to obtain better responses.⁶

Due to limitations of the currently available ERT, alternative treatment strategies are being investigated.⁷ A new approach in PD is substrate reduction therapy (SRT) to reduce glycogen synthesis. Inhibiting the Gys1 isoform of glycogen synthase is an attractive target to reduce glycogen availability for glyophagy. The appeal is enhanced by reports that cytosolic glycogen synthesis is increased in a mouse model of PD, mediated by an increase in several glycogenic pathway proteins including Gys1.^{8–10} The utility of this SRT approach was first demonstrated in a mouse model in which the disruption of Gys1 in Gaa-null animals restored muscle function.¹¹ More recently, administration of a small molecule inhibitor of GYS1¹⁰ or antisense oligonucleotide-mediated Gys1 knockdown¹² reduced glycogen accumulation in a mouse model of PD. In our studies, we tested the utility of an SRT strategy (Fig-

ure 1A) that inhibits glycogen synthesis via decreases in Gys1 enzyme using a novel CD71 Centyrin:Gys1 siRNA conjugate (Figure 1B).

Centyrins are small, engineered proteins derived from human Tenascin C, a protein found in the extracellular matrix.¹³ Centyrins are ~10K Da proteins with high receptor binding affinity and specificity like antibodies. Centyrins are produced in *E. coli* as soluble proteins with no disulfide linkages, no glycosylation, and no Fc domains leading to a highly stable homogeneous protein. Centyrins are produced with a single Cysteine selectively introduced distal from the binding site that can be site-specifically conjugated to produce homogeneous conjugates with a defined Oligonucleotide to Centyrin ratio of 1 (OCR1). From a library of trillions of created variants, CD71 Centyrin was chosen for this study. This Centyrin binds with high specificity and affinity to CD71, transferrin receptor type 1, which is highly expressed in muscle. Once bound, Centyrin conjugated to Gys1 siRNA is internalized

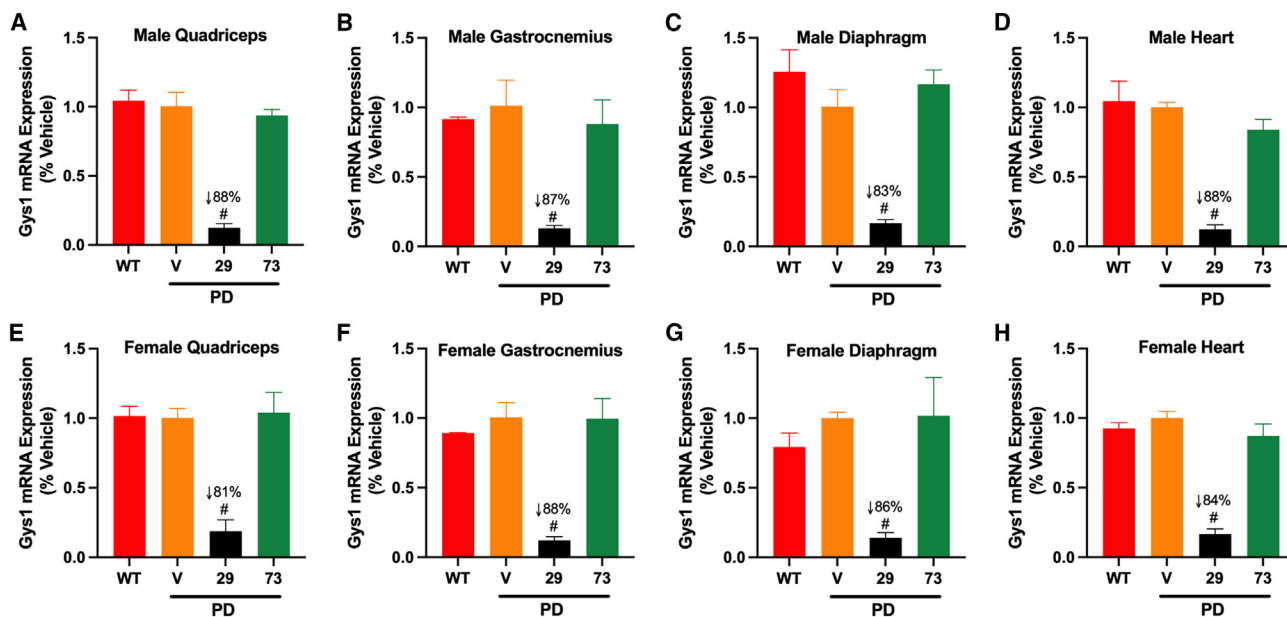


Figure 2. ABXC-29 treatment reduces *Gys1* mRNA levels in muscle

Gys1 mRNA expression was measured with qPCR in quadriceps, gastrocnemius, diaphragm, and heart harvested 6 months after treatment initiation from male (A–D) and female (E–H) WT mice treated with vehicle (WT, red bars), and $6^{neo}/6^{neo}$ mice treated with vehicle (V, orange bars), ABXC-73 (73, green bars), or ABXC-29 (29, black bars). All data are expressed as mean (SD). $n = 3$. One-way ANOVA with Tukey's multiple comparison test. # $p < 0.005$ vs. all other groups.

into the cell where it binds to the RISC complex and hybridizes to *Gys1* mRNA resulting in gene knockdown.¹³ The CD71 Centyrin and *Gys1* siRNA used in this study are specific for the murine forms of CD71 and *Gys1*. This Centyrin does not bind to the apical domain of CD71, which is thought to be needed for brain penetration. However, the human-specific molecule that is currently in clinical trials is not competitive with transferrin and binds the apical domain, which may enable transport across the blood brain barrier.

To test the efficacy of this Centyrin targeting and delivery platform in PD, we utilized the well-characterized mouse model, $6^{neo}/6^{neo}$, which exhibits features of both IOPD and LOPD.¹⁴ Treated mice were tested for impact on glycogen metabolism as well as functional performance. We found that treatment with the CD71 Centyrin:*Gys1* siRNA conjugate significantly reduced glycogen accumulation in quadriceps, gastrocnemius, diaphragm, and heart. Further, impaired treadmill performance was restored in male mice and cardiomegaly was reduced in female mice.

RESULTS

ABXC-29 treatment reduces glycogen synthesis

ABXC-29 treatment reduces *Gys1* mRNA levels in skeletal and cardiac muscle

To determine efficacy of ABXC-29 on *Gys1* gene knockdown, *Gys1* mRNA levels were monitored in male and female quadriceps, gastrocnemius, diaphragm, and heart harvested 6 months after treatment initiation. *Gys1* mRNA levels were reduced by more than 80% compared with vehicle-treated $6^{neo}/6^{neo}$ mice in quadriceps

(Figures 2A and 2E), gastrocnemius (Figures 2B and 2F), diaphragm (Figures 2C and 2G), and heart (Figures 2D and 2H) indicating the potency of the CD71 Centyrin:*Gys1* siRNA conjugate at *Gys1* gene silencing in skeletal and cardiac muscle.

ABXC-29 treatment reduces GYS1 protein levels in skeletal and cardiac muscle

GY51 protein expression was monitored via immunoblot to measure effects of ABXC-29 3, 6, and 9 months after initiation of treatment. In quadriceps (Figures 3A and 3E), GYS1 protein levels were significantly elevated (70% in males, 150% in females) in $6^{neo}/6^{neo}$ mice treated with vehicle or scrambled siRNA as compared with wild type (WT). A similar trend was observed in gastrocnemius (Figures 3B and 3F) and heart (Figures 3C and 3G), in some cases reaching statistical significance. ABXC-29 treatment reduced GYS1 protein expression in quadriceps (Figures 3A and 3E), gastrocnemius (Figures 3B and 3F), and heart (Figures 3C and 3G) $\geq 97\%$ compared with vehicle or scrambled-treated $6^{neo}/6^{neo}$ mice correlating with decreased *Gys1* mRNA levels (Figure 2). In brain (Figures 3D and 3H), no reduction in GYS1 protein expression was observed, indicating, as expected, lack of efficacy of the CD71 Centyrin:*Gys1* siRNA conjugate in this organ. These data are consistent with data reported by other groups.^{15–18}

ABXC-29 reduces GYS1 enzymatic activity in skeletal and cardiac muscle

Glycogen synthase enzymatic activity was measured in quadriceps, gastrocnemius, heart, and brain 3, 6, and 9 months after treatment

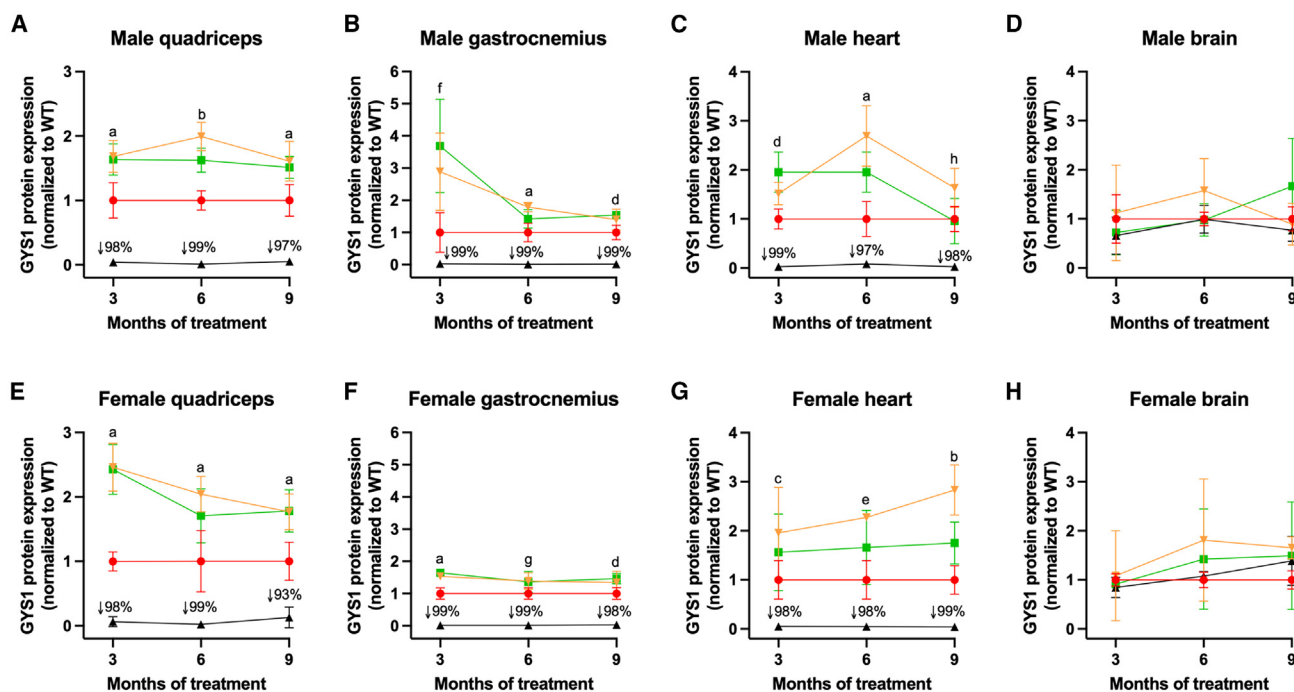


Figure 3. ABXC-29 treatment reduces GYS1 protein levels in muscle

GYS1 protein expression was monitored with western blot in quadriceps, gastrocnemius, heart, and brain harvested from male (A–D) and female (E–H) WT mice treated with vehicle (red circles), and $6^{neo}/6^{neo}$ mice treated with vehicle (V, orange inverted triangles), ABXC-73 (negative control, green squares), or ABXC-29 (active compound, black triangles) 3, 6, and 9 months after treatment initiation. Percent decrease of 29 compared with V is indicated. All data are expressed as mean (SD). $n = 3–5$. One-way ANOVA with Tukey's multiple comparison test. Statistical analysis compares all groups at a given length of treatment. ^a $p < 0.05$ for comparison of each group with every other group except V vs. 73, ^b $p < 0.05$ for comparison of each group with every other group, ^c $p < 0.05$ for comparison of 29 vs. V and 73, ^d $p < 0.05$ for comparison of each group with every other group except V vs. 73 and WT vs. V, ^e $p < 0.05$ for comparison of each group with every other group except 73 vs. WT and V, ^f $p < 0.05$ for comparison of each group with every other group except WT vs. V and 29 and V vs. 73, ^g $p < 0.05$ for comparison of each group with every other group except WT vs. V and 73 and V vs. 73, and ^h $p < 0.05$ for comparison of 29 vs. other groups. Representative images of western blots shown in Figure S1.

initiation. GYS1 enzymatic activity measured 3 months after treatment, in the presence of added glucose-6-P, was elevated (58%–87%) in male quadriceps (Figure 4A), gastrocnemius (Figure 4B), and heart (Figure 4C) from $6^{neo}/6^{neo}$ mice treated with scrambled siRNA or vehicle. This elevation continued at 6 and 9 months in male muscle. A similar trend for elevated GYS1 enzymatic activity, in some cases reaching statistical significance, was observed in female muscle tissues 3, 6, and 9 months after initiation of treatment (Figures 4E–4G). Treatment with ABXC-29 decreased enzymatic activity 81%–97% in male and female quadriceps (Figures 4A and 4E), gastrocnemius (Figures 4B and 4F), and heart (Figures 4C and 4G) but had no effect in brain (Figures 4D and 4H), consistent with decreased GYS1 protein expression (Figure 3). Glycogen synthase activity measured in the absence of the allosteric effector, glucose-6-P, was not elevated in $6^{neo}/6^{neo}$ mice compared with WT, while treatment with ABXC-29 inhibited activity 74%–92% in muscle, but not brain (Figure S2). The activity ratio, which provides an index of the percent of active GYS1, suggested a trend for GYS1 to be less active in muscle from $6^{neo}/6^{neo}$ mice as compared with WT (Figure S3).

ABXC-29 treatment reduces glycogen levels in skeletal and cardiac muscle

Glycogen levels were monitored biochemically in quadriceps, gastrocnemius, diaphragm, heart, brain, and liver 3, 6, and 9 months after treatment began. In all tissues, except for liver, glycogen levels were significantly elevated in $6^{neo}/6^{neo}$ mice, regardless of treatment, as compared with WT controls (Figure 5). ABXC-29-mediated reduction of glycogen occurred in quadriceps, gastrocnemius, diaphragm, and heart. In quadriceps, female glycogen levels (Figure 5D) were reduced 30%–40% compared with vehicle-treated $6^{neo}/6^{neo}$ mice at all times tested, while males (Figure 5A) first showed a statistically significant decrease after 6 months of treatment. Gastrocnemius glycogen in female (Figure 5E) and male mice (Figure 5B) was reduced 34%–63% by ABXC-29 treatment. Heart glycogen levels in male $6^{neo}/6^{neo}$ mice (Figure 5G) after 3 months of treatment were reduced ~30% and remained at this reduced level at 6 and 9 months after treatment. In contrast, heart glycogen levels in ABXC-29 treated female mice (Figure 5J) resembled vehicle-treated mice after 3 months of treatment but after 9 months of treatment were decreased ~40% compared with 3-month levels. Heart weight, normalized to body weight, after 9 months of treatment was reduced in female (Figure S4)

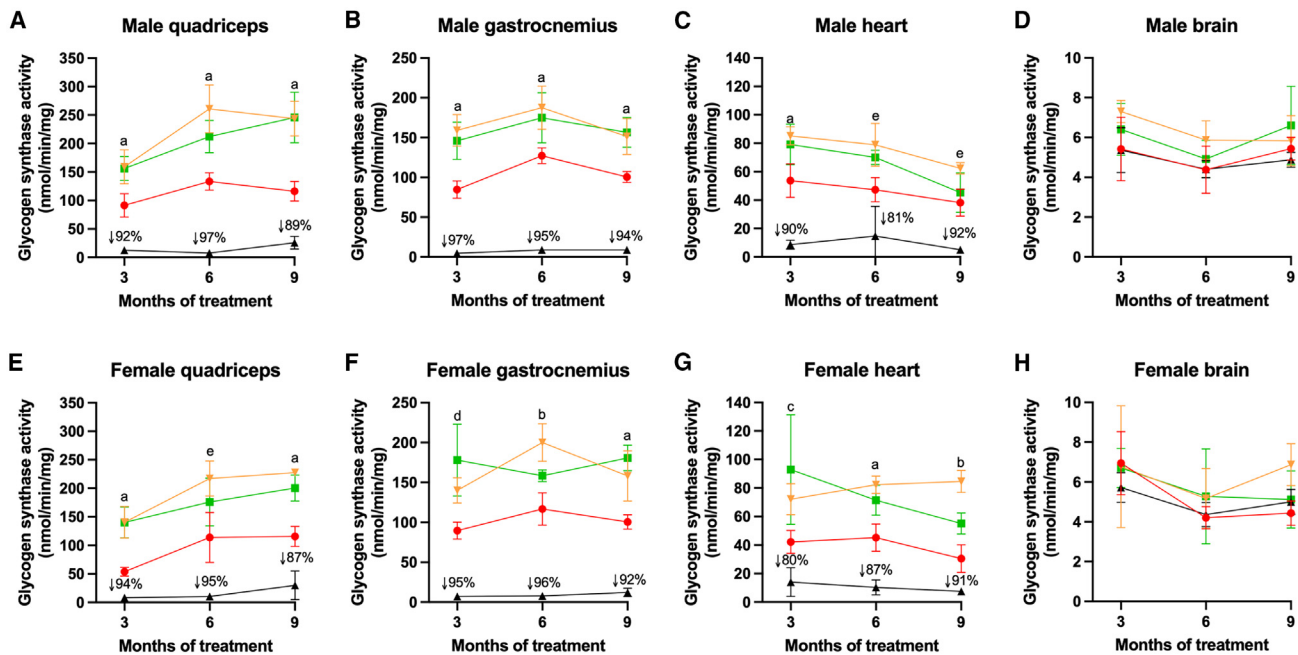


Figure 4. ABXC-29 treatment reduces GYS1 enzymatic activity levels in muscle but not brain

Glycogen synthase enzymatic activity was measured in tissues harvested from male (A–D) and female (E–H) WT mice treated with vehicle (red circles), and 6^{neo}/6^{neo} mice treated with vehicle (V, orange inverted triangles), ABXC-73 (negative control, green squares), or ABXC-29 (active compound, black triangles) 3, 6, and 9 months after treatment initiation. Percent decrease of 29 compared with V is indicated. All data are expressed as mean (SD). $n = 3–5$. One-way ANOVA with Tukey's multiple comparison test. Statistical analysis compares all groups at a given length of treatment. ^a $p < 0.05$ for comparison of each group with every other group except V vs. 73, ^b $p < 0.05$ for comparison of each group with every other group, ^c $p < 0.05$ for comparison of each group with every other group except WT vs. V and 29 and V vs. 73, ^d $p < 0.05$ for comparison of each group with every other group except V vs. 73 and WT vs. V, ^e $p < 0.05$ for comparison of each group with every other group except 73 vs. WT and V.

but not male 6^{neo}/6^{neo} mice (data not shown). Diaphragm glycogen in female mice (Figure 5F) showed a similar pattern to female heart, while male diaphragm glycogen (Figure 5C) was consistently reduced >50% at all durations of treatment. Liver glycogen levels were similar in all groups (Figures 5I and 5L). Brain glycogen levels in males (Figure 5H) were not reduced by ABXC-29 treatment while an ~30% increase was observed in females (Figure 5K) after 6 months of treatment, which subsided at 9 months. Taken together, these results indicate the efficacy of ABXC-29 at reducing glycogen levels in cardiac and skeletal muscle. Lack of a treatment effect with ABXC-29 in liver was expected due to the expression of the *Gys2* isoform of glycogen synthase in this tissue.

ABXC-29 treatment does not improve muscle pathology

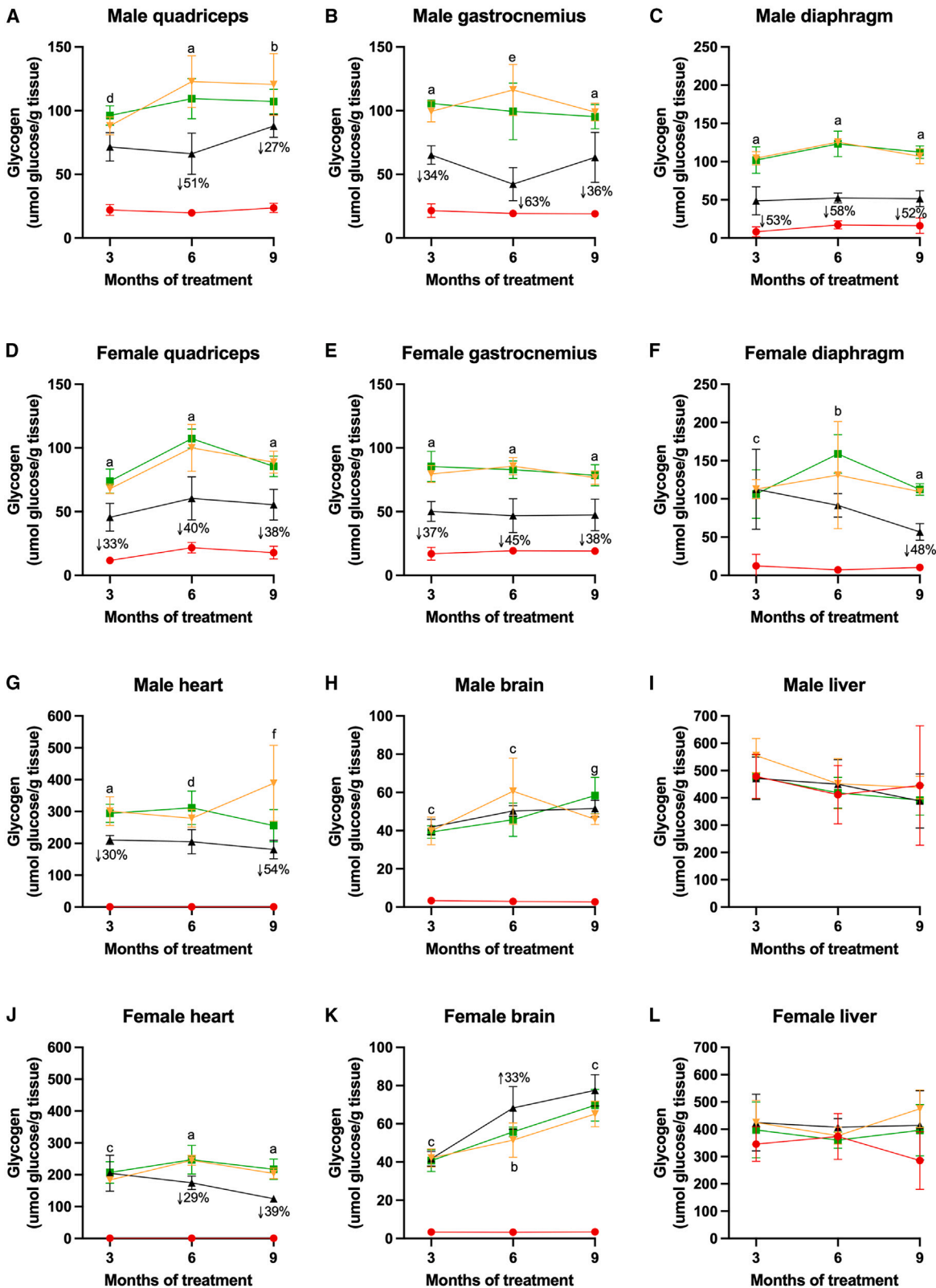
Quadriceps sections were evaluated for vacuolization (representing lysosomal glycogen accumulation) after 3, 6, and 9 months of treatment. Accumulation of glycogen was observed in myocytes (Figures 6E and 6F), vascular smooth muscle (Figures 6G and 6I), and Schwann cells (Figures 6H and 6I) from 6^{neo}/6^{neo} mice. The average vacuolization and PAS scores for all 6^{neo}/6^{neo} mice, regardless of treatment were elevated compared with WT mice and treatment with ABXC-29 did not reduce scores (Figures 6J–6M). These data indicate that glycogen reduction by ABXC-29 did not improve vacuolization representing lysosomal glycogen accumulation.

ABXC-29 treatment has mixed effects on functional performance

Body weight for all groups of male mice (Figure 7A) were similar over the course of the study while female WT mice were heavier than female 6^{neo}/6^{neo} mice regardless of treatment (Figure 7D). To determine efficacy of ABXC-29 treatment on neuromuscular function, mice were subjected monthly to grip strength, wire hang, and rotarod. Grip strength of 6^{neo}/6^{neo} male and female mice was impaired, compared with WT mice throughout the course of the study (Figures 7B and 7E). Similarly, wire hang analysis revealed stable performance of WT mice over time, with 6^{neo}/6^{neo} showing a trend toward impairment for females (Figure 7F) and dramatic impairment in males (Figure 7C). 6^{neo}/6^{neo} mice were also impaired compared with WT mice as assessed by rotarod, to a more significant extent in male (Figure 7G) than female mice (Figure 7I), with a trend toward improvement in males treated with ABXC-29 at later times tested. Treadmill exercise performance measured after 8 months of treatment showed no effects of disease or treatment in female mice (Figure 7J); however, male 6^{neo}/6^{neo} mice were significantly impaired compared with WT mice and ABXC-29 treatment restored performance to WT levels (Figure 7H).

DISCUSSION

Here we showed the efficacy of a novel platform, a CD71 Centyrin:siRNA conjugate, to deliver *Gys1* siRNA to skeletal and



(legend on next page)

cardiac muscle and reduce glycogen accumulation in a mouse model of PD. The CD71-Centyrin:siRNA conjugate mechanism is to lower muscle glycogen levels by reducing the production of new glycogen; existing lysosomal glycogen will not be affected by this approach. In addition, since these mice lack any GAA activity, it may require an extended treatment period to yield the maximum glycogen knockdown (see Figure 1). Administration of CD71 Centyrin:*Gys1* siRNA conjugate (ABXC-29), which binds the transferrin type 1 receptor, effectively reduced *Gys1* mRNA, GYS1 protein and enzymatic activity, and glycogen levels in quadriceps, gastrocnemius, diaphragm, and heart. No effects were seen on liver glycogen metabolism highlighting the siRNA selectivity for the *Gys1* vs. the *Gys2* isoform of glycogen synthase.

The utility of Centyrins as a targeting and delivery strategy for siRNA was first demonstrated by Klein et al.¹³ in studies targeting tumor EGFR-expressing tumor cells. For this study, a surrogate Centyirin that binds murine CD71 and an siRNA that recognizes murine GYS1 were required. While the properties of the Centyirin murine surrogate enable efficient siRNA uptake in muscle, we anticipate that binding that is competitive with respect to transferrin is likely to preclude efficient brain delivery.¹⁷

The $6^{neo}/6^{neo}$ mouse model used in these studies has no GAA activity, replicating the most severe form of PD. Glycogen levels in these mice are elevated in several tissues at or soon after birth and progressively increase over time in heart, brain, diaphragm, and type II skeletal muscle.¹⁹ Glycogen levels appear to plateau by ~4 months of age, except for diaphragm. This is the age when treatment was initiated in our current study. Therefore, the significant reduction (~30%–60%) of glycogen stores we observed even under this worst-case scenario, supports the potential of this therapeutic approach. However, despite this significant reduction, glycogen levels in ABXC-29-treated PD mice remained higher than WT throughout the course of the study in all muscle tissues tested. Except for female heart and diaphragm, in which glycogen levels were progressively decreasing, the amount of glycogen reduction is relatively constant 3, 6, and 9 months after treatment. This suggests that, at least in male mice, the maximal glycogen reduction with this approach was reached. We have seen *Gys1* mRNA knockdown in skeletal muscle as early as 2 weeks after dosing with ABXC-29 (data not shown). The effects of ABXC-29 treatment on GYS1 protein and enzyme activity over time suggest that increasing treatment frequency would not significantly increase efficacy; notably, even with the increased length of time (2 months, see timeline in Figure 8) between last treatment and tissue harvest 9 months after treatment initiation, GYS1 protein levels and enzyme

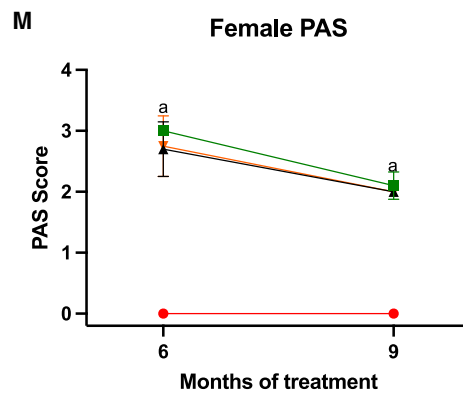
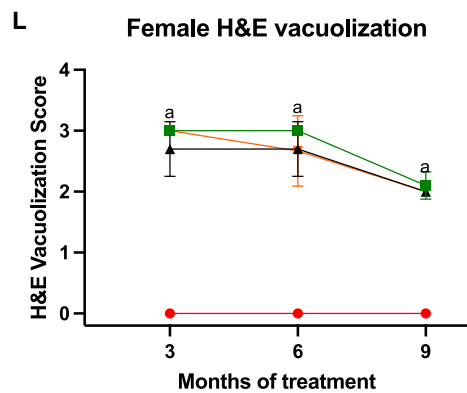
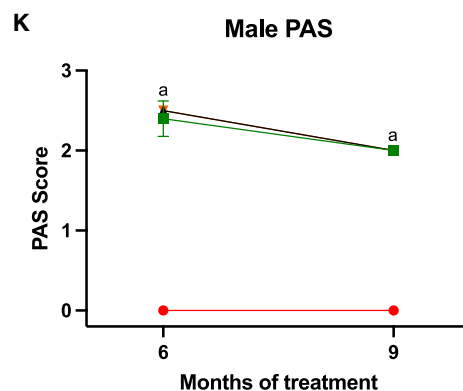
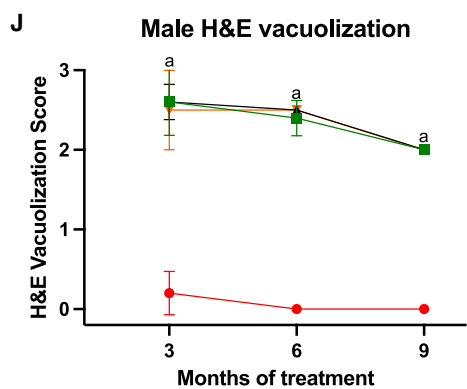
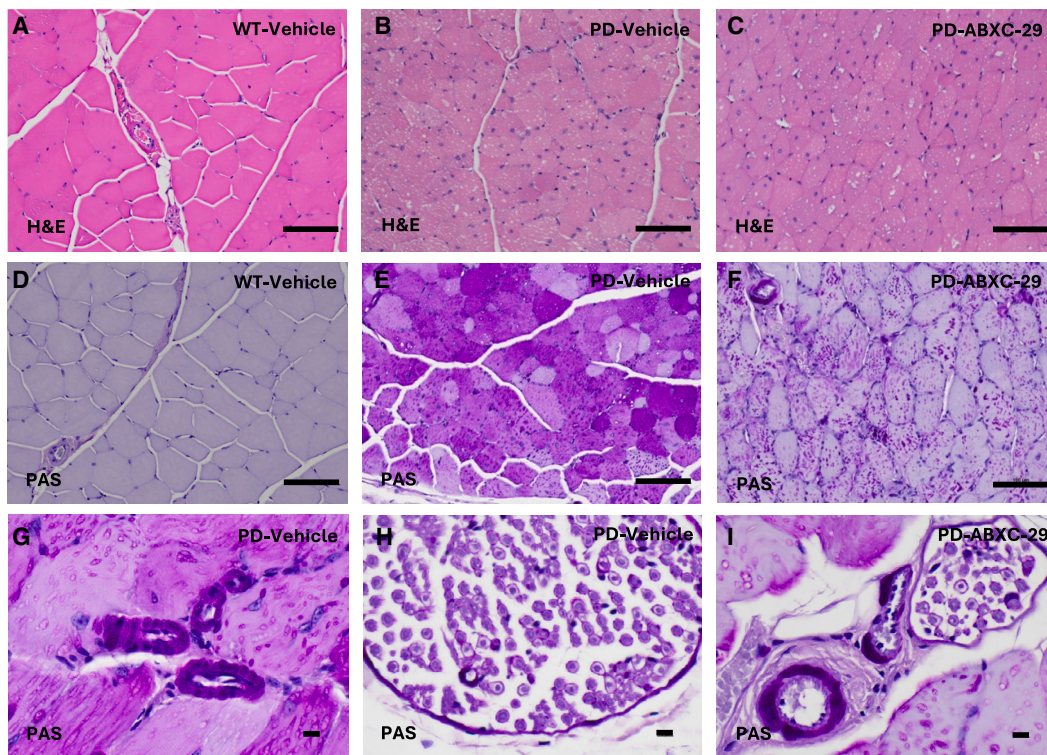
activity remained reduced 87%–99% in muscle tissues. Ullman et al.,¹⁰ using a small molecule inhibitor of GYS1, and Weiss et al.,¹² using a *Gys1* antisense oligonucleotide, reported comparable glycogen reductions to what we report here. Using metabolic tracer analysis in $6^{neo}/6^{neo}$ mice, Ullman et al.¹⁰ reported that 8 and 12 weeks were required to clear 95% of glycogen in gastrocnemius muscle lacking GAA. In contrast, the half-life of glycogen in gastrocnemius from mice expressing GAA was about 16 h. This observation coupled with the greater than 95% inhibition of GYS1 activity observed in skeletal muscle with ABXC-29 suggests that we should see very little glycogen remaining after even 3 months of treatment. However, it is clear using histology and biochemical measurements that significant lysosomal glycogen stores remain. This residual glycogen may be cleared by ERT or in patients who have some level of GAA activity. Consideration of the biochemical and histology data together suggests that the reduction of glycogen measured biochemically can be attributed to cytosolic reduction and lysosomal glycogen turnover is very slow. However, methods that can quantitatively distinguish cytosolic and lysosomal glycogen stores would be required to answer this fully.

We observed increased GYS1 protein expression and glycogen synthase activity in muscle of $6^{neo}/6^{neo}$ mice as compared with WT controls. This seemingly counterproductive adaptation has also been reported in whole or in part by others. Taylor et al.⁹ observed unchanged *Gys1* mRNA levels, elevated GYS1 protein expression, and elevated GYS1 enzymatic activity in the presence of glucose-6-P in $6^{neo}/6^{neo}$ mice. Canibano-Fraile et al.⁸ reported that GYS1 protein expression was elevated in 60-week-old $6^{neo}/6^{neo}$ mice. A trend for increase of GYS1 protein expression was also observed in $6^{neo}/6^{neo}$ mice by Ullman et al.¹⁰ with a significant increase in phosphorylated GYS1. In a small group of five human subjects with PD, no elevation of GYS1 protein expression was observed in one study⁸; however, in a separate study we found that Pompe patients had an elevated level of *Gys1* protein vs. healthy (Mark Tarnopolsky, personal communication).

Sex differences were observed in both our functional and biochemical studies, but not for *Gys1* mRNA or protein decreases with ABXC-29. Male mice with PD were more impaired on wire hang, rotarod, and treadmill than female mice with the disease. This was seen most dramatically in treadmill studies with the disease causing no impairment in females but significant impairment in males. Glycogen reduction mediated by ABXC-29 treatment in female heart and diaphragm was progressive over the 9 months monitored, while in males, maximal reduction was observed after 3 months of treatment and

Figure 5. ABXC-29 treatment reduces glycogen levels in heart but not brain or liver

Glycogen concentration was measured biochemically in tissues harvested from male (A–C and G–I) and female (D–F and J–L) WT mice treated with vehicle (red circles), and $6^{neo}/6^{neo}$ mice treated with vehicle (V, orange inverted triangles), ABXC-73 (negative control, green squares), or ABXC-29 (active compound, black triangles) 3, 6, and 9 months after treatment initiation. Percent change of 29 compared to V is indicated. All data are expressed as mean (SD). $n = 3–5$. One-way ANOVA with Tukey's multiple comparison test. Statistical analysis compares all groups at a given length of treatment. ^a $p < 0.05$ for comparison of each group with every other group except V vs. 73, ^b $p < 0.05$ for comparison of each group with every other group except 73 vs. V and 29, ^c $p < 0.05$ for comparison of WT vs. every other group, ^d $p < 0.05$ for comparison of each group with every other group except V vs. 73 and 29, ^e $p < 0.05$ for comparison of each group with every other group except 29 vs. WT and V vs. 73, ^f $p < 0.05$ for comparison of each group with every other group except 73 vs. 29, ^g $p < 0.05$ for comparison of each group with every other group except 29 vs. V and 73.



(legend on next page)

maintained. This difference occurred even though reductions of GYS1 protein expression and enzymatic activity in heart were maximally reduced by 3 months in both sexes. Similar measurements were not done in diaphragm due to tissue availability. A reduction in heart size relative to body weight was only observed in female mice. Perigonadal fat pads in female mice, but not male mice, as a percent of body weight were lower in $6^{neo}/6^{neo}$ mice as compared with WT after 9 months of treatment (2.50 ± 0.32 (WT), 1.25 ± 0.12 (V), 1.25 ± 0.21 (73), 1.36 ± 0.21 (29), $p < 0.05$). Further studies would be required to identify the mechanism(s) explaining these intriguing sex differences. Human opposite-sex siblings with the same mutation(s) have been observed to exhibit different phenotypes.²⁰

While it may appear that there is discrepancy between the reduction of GYS1 and limited improvement of pathological and functional outcomes, the reduction of muscle glycogen we observed is maximally ~60% compared with untreated diseased mice, which is still dramatically elevated compared with normal levels. The reduction of GYS1 protein and enzyme activity is greater than 87% in muscle, indicating robust inhibition in this tissue by ABXC-29. However, the mouse model used in these studies completely lacks GAA activity. Therefore, while treatment with ABXC-29 dramatically reduces the amount of “new” cytosolic glycogen available to accumulate in lysosomes, glycogen accumulated in lysosomes prior to ABXC-29 treatment remains unable to be broken down, as we observed by histological techniques. However, ABXC-29 treatment in LOPD, where residual GAA remains, or in IOPD, in combination with ERT, would have the potential to produce a more robust functional and pathological outcome by both removing accumulated lysosomal glycogen and reducing glycogen that is available to be degraded through glycolysis. One potential strategy in patients would be to first lower lysosomal glycogen load with ERT and then maintain these levels with SRT. This would result in a respite from infusion, thereby improving patient quality of life. Another factor for interpreting the modest functional improvements with ABXC-29 treatment is the role of brain glycogen accumulation in PD. ABXC-29 lacks efficacy in brain; a tissue in which CNS-specific glycogen reduction in a Pompe mouse model improved functional performance.²¹ The reason for lack of efficacy in the CNS is being investigated and appears to be related to the nature of binding of murine Centyrin surrogate to the transferrin receptor. Potentially a Centyrin with different binding properties could provide efficacy to this currently non-responsive tissue.

The effects of reducing glycogen synthetic ability have been investigated in mice in both a whole body *Gys1* knockout model and an adult

muscle-specific *Gys1* knockdown. The expectation was impaired glucose tolerance and impaired exercise performance. In the first model, no impairments in either were reported.^{22,23} However, these mice went through fetal development lacking GYS1, with 90% dying shortly after birth,²⁴ and adults had changes in muscle fiber type.²³ In addition, in the former study, brain glycogen was absent while in the current study brain GYS1 was not reduced. These factors may limit the applicability of those findings to our current study in which inhibition does not begin until adulthood. In contrast, the muscle-specific *Gys1* knockdown model exhibited both impaired glucose tolerance and treadmill performance.²⁵ In our current study, reducing GYS1 in the $6^{neo}/6^{neo}$ mice had no effect on treadmill performance in females and improved performance in males. We did not monitor glucose tolerance in our study; however, knockout of *Gys1* in the $6^{neo}/6^{neo}$ background restored glucose tolerance to normal levels¹¹ mitigating concern that impaired glucose tolerance could result from reducing glycogen synthetic capacity in muscle. In addition, improved glucose tolerance and whole-body insulin resistance was improved in Pompe mice by reducing GYS1 with a small molecule inhibitor.²⁶ The translatability to humans of this substrate reduction approach was recently discussed.¹⁰ The favorable tolerability of reduced glycogen stores observed in patients with PP1r3A mutations is encouraging.^{10,27} It is unclear how the greater muscle, as compared with liver, glycogen stores in human vs. mouse will influence tolerability.²³ The lack of impact of SRT on brain glycogen stores limits concerns about potential negative impacts in this organ but does not reduce the high glycogen levels that accumulate in the PD brain.

While ERT with rhGAA reduces muscle glycogen content in PD, it is ineffective in the brain. CNS-specific reduction of glycogen with gene therapy was reported to improve rotarod performance in $6^{neo}/6^{neo}$ mice,²¹ while monotherapy with a small molecule inhibitor of GYS1¹⁰ or ABXC-29 did not, indicating the role of the CNS in the disease pathology. Despite the ubiquitous expression of the transferrin receptor, to which the CD71 is targeted, we did not observe a reduction in glycogen synthase protein or glycogen in brain with ABXC-29, likely due to the epitope for the murine surrogate Centyrin. Further studies will be required to determine if apical binding is required for efficacy in neural tissue.

In conclusion, ABXC-29 reduced *Gys1* mRNA, GYS1 protein expression, and GYS1 enzymatic activity greater than 80% in skeletal and cardiac muscle in a mouse model of PD when treatment was initiated at 4 months of age. This resulted in a 30%–60% decrease in glycogen concentration in these tissues and was well tolerated with no toxicity associated with the reduction of GYS1.

Figure 6. ABXC-29 treatment does not reduce vacuolization, i.e., lysosomal glycogen, in quadriceps

Following treatment for 3, 6, or 9 months, quadriceps were harvested from WT mice treated with vehicle (A and D; representative sections after 6 months of treatment), and $6^{neo}/6^{neo}$ (PD) mice treated with vehicle (B, E, G, and H; representative sections after 6 months of treatment), and ABXC-29 (C, F, I; representative sections after 6 months of treatment) and scored (J, K, L, and M), as described in materials and methods. H&E (A–C) and PAS (D–I) staining. Note glycogen accumulation in vascular smooth muscle cells in vehicle (G) and ABXC-29 (I) treated $6^{neo}/6^{neo}$ mice and Schwann cells in vehicle (H) and ABXC-29 (I) treated $6^{neo}/6^{neo}$ mice. All data are expressed as mean (SD). $n = 3–5$. One-way ANOVA with Tukey’s multiple comparison test ^a $p < 0.05$ for comparison of WT vs. every other group. (A)–(F): scale bar, 100 μ m, total magnification $\times 200$. (G)–(I): scale bar, 10 μ m, total magnification $\times 600$.

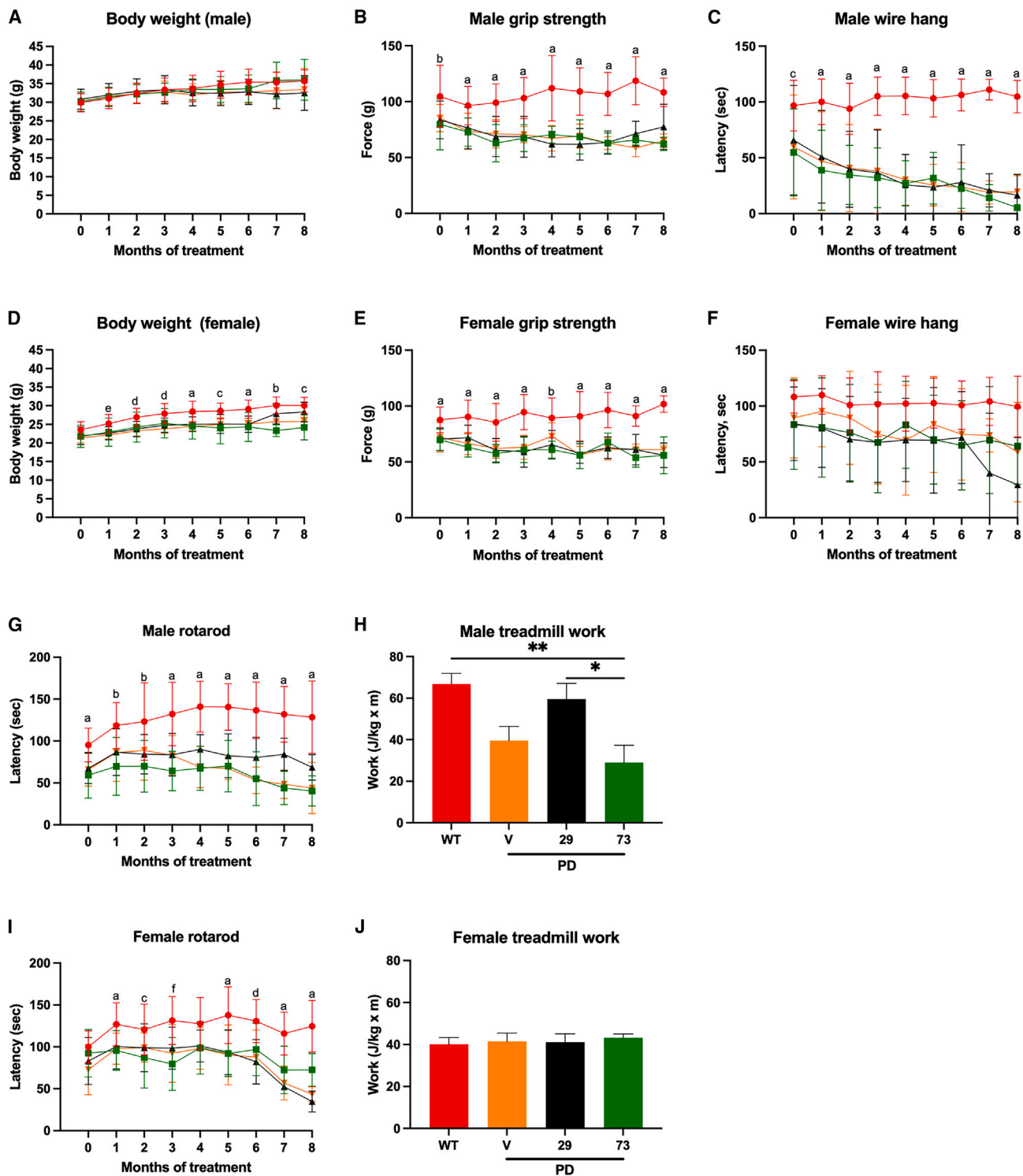


Figure 7. ABXC-29 treatment does not mitigate GS, WH, or RR impairment but improves male treadmill performance

Body weight, grip strength, wire hang, and rotarod performance were monitored monthly and treadmill performance monitored 8 months after treatment initiation in male (A–C, G, and H) and female (D–F, I, and J) WT mice treated with vehicle (red circles), and $\delta^{neo}/\delta^{neo}$ mice treated with vehicle (V, orange inverted triangles), ABXC-73

(legend continued on next page)

These studies indicate that a CD71 Centyrin:*Gys1* siRNA conjugate is a promising modality for the treatment of patients with PD, either as a monotherapy in LOPD patients with sufficient, but lower levels of endogenous GAA activity, or perhaps using combination therapy with rhGAA ERT to reduce existing lysosomal glycogen load and ABCX-29 to inhibit cytosolic glycogen synthesis and its uptake and accumulation into lysosomes. This combination could potentially reduce the frequency of multiple-hour biweekly infusions, anaphylactic shock, and lead to improved patient outcomes.

MATERIALS AND METHODS

Mouse model

$6^{neo}/6^{neo}$ mice, a model of PD,¹⁴ and WT mice with the same genetic background were purchased from Jackson Laboratories (strain #004154). $6^{neo}/6^{neo}$ mice are homozygous for disruption of the acid alpha-glucosidase gene (*Gaa*). Mice were housed (12 h light/dark cycle) in temperature and humidity-controlled rooms with constant access to both food (18% protein diet [Envigo, T20185X]) and water (type 3) throughout the duration of the experiment. All procedures were approved by Ball State University Animal Care and Use Committee.

Experimental design

Baseline functional measurements (described below) were made on 4-month-old male and female $6^{neo}/6^{neo}$ and WT mice prior to treatment. After these measurements, treatment was administered every 28 days (described below) (Figure 8A). Grip strength, wire hang, and rotarod were conducted monthly. Treadmill performance was monitored 8 months after treatment was initiated. Tissue was harvested 3, 6, and 9 months after treatment initiation to measure *Gys1* mRNA, protein, enzyme activity, and glycogen.

Treatment

Treatment was delivered intravenously (lateral tail vein). WT mice were injected with vehicle (25 mM HEPES, 150 mM NaCl, pH 7.4; 3.33 mL/kg body weight) to serve as a control (treatment group WT) (Figure 8B). One group of $6^{neo}/6^{neo}$ mice was injected with vehicle (treatment group V). Another $6^{neo}/6^{neo}$ group was injected with CD71 Centyrin:*Gys1* siRNA conjugate (ABXC-29; 17.8 mg/kg body weight, treatment group 29). A last group of disease model mice was injected with CD71 Centyrin:scrambled siRNA conjugate (ABXC-73; 17.8 mg/kg body weight, treatment group 73).

Functional studies

Wire hang

Mice were placed on a wire grid that was gently waved three times before inverting 30 cm above a cushioned surface. Each mouse was allowed a maximum of 120 s to remain on the grid and 60 s to rest between each of the three trials. Average latency was calculated.

Grip strength

To test forearm grip strength, mice were held by the base of the tail and pulled horizontally while forepaws gripped testing bars (Linton Instruments). The average grip strength for both forearms over three trials was calculated.

Rotarod

Mice were tested on a six-lane rotarod (Maze Engineers) set to accelerate from 4 to 40 rpm over 180 s. Latency was determined by mice meeting the earliest occurrence of one of the following criteria. First, passive rotation, in which mice gripped the rod and completed two full rotations without falling. Second, mice fell from the rotarod. Third, mice remained on the rod for 180 s. Mice were subjected to three trials and were returned to their cage for 5 min between each trial. Average latency was calculated for the three trials.

Treadmill

Mice underwent 2 consecutive training days followed by 2 days of rest and then were tested on a five-lane mouse treadmill (Maze Engineers). Training days consisted of 17 min total on the treadmill with 2 min to explore without the belt moving, 5 min at 3 m/min, 5 min at 6 m/min, and the last 5 min at 9 m/min. During training and testing, the treadmill was set to a 20-degree incline and a 1.2 mA current was applied to the electrical grid at the bottom of the instrument. Sound (120 db) and light (10,000 Lux) stimuli were implemented to encourage running when the mice were in the fatigue zone (mouse on shock grid or base of tail at belt/shock grid interface) for 2 or more seconds. On the testing day, parameters were as follows: 5 min at 3 m/min, 5 min at 6 m/min, 20 min at 9 m/min, 15 min at 15 m/min, 15 min at 21 m/min, and 60 min at 27 m/min. Latency was determined by mice meeting the earliest incidence of one of the following criteria: running for 120 min, remaining in the fatigue zone for 10 s, or remaining on the shock grid for 10 s. Work (J) was calculated as follows: body weight (kg) \times running speed (m/min) \times running time (min) \times incline \times 9.8 (J/kg \times m).

Tissue harvest

All tissues were harvested in the morning from fed mice euthanized via cervical dislocation. Tissue harvested for glycogen, glycogen synthase activity, and GYS1 protein expression analysis were immediately frozen in liquid nitrogen and stored at -80°C . Tissue harvested for *Gys1* mRNA expression was placed in RNAlater. Quadriceps for histological evaluation was placed in 10% neutral-buffered formalin (NBF) for 48–72 h at room temperature and then transferred to 10% NBF containing 1% periodic acid (4 g) for 48 h at 4°C .²⁸ After washing in PBS for 10 min at room temperature three times, tissue was moved to 70% ETOH and paraffin sections prepared and stained with hematoxylin and eosin (H&E) or Periodic acid-Schiff (PAS; Indiana University School of Medicine Histology Core).

(negative control, green squares), or ABXC-29 (active compound, black triangles). All data are expressed as mean (SD). $n = 3-15$. One-way ANOVA with Tukey's multiple comparison test. Statistical analysis compares all groups at a given length of treatment. ^a $p < 0.05$ for comparison of WT vs. every other group, ^b $p < 0.05$ for comparison of WT vs. 29 and 73, ^c $p < 0.05$ for comparison of WT vs. 73, ^d $p < 0.05$ for comparison of WT vs. 29 and V, ^e $p < 0.05$ for comparison of WT vs. V, ^f $p < 0.05$ for comparison of WT vs. V and 73, ^g $p < 0.05$ vs. 73, ^h $p < 0.05$ vs. WT.

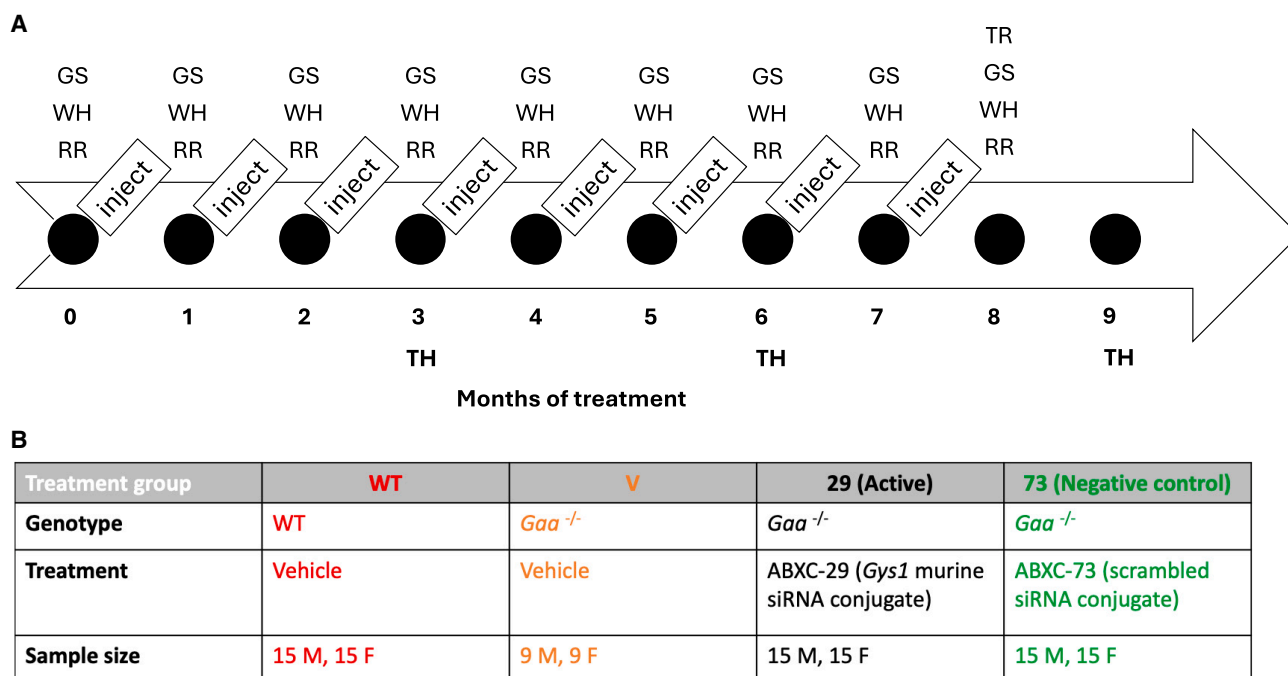


Figure 8. Experimental timeline and treatment groups

(A) Mice were injected every 28 days and grip strength (GS), wire hang (WH), and rotarod (RR) performance were monitored monthly. Treadmill (TR) performance was monitored 8 months after treatment was initiated. Tissue harvest (TH) occurred 3, 6, and 9 months after treatment initiation and *Gys1* mRNA expression, GYS1 protein expression, GYS1 enzymatic activity, and glycogen concentration were measured in several tissues. (B) Treatment groups comprised 4-month-old male and female *Gaa* disrupted mice ($6^{neo}/6^{neo}$) that were injected with vehicle or Centyrin conjugated to either *Gys1* siRNA (ABXC-29) or scrambled siRNA (ABXC-73). Wild-type mice were injected with vehicle.

Histological analysis

H&E-stained paraffin sections contained numerous vacuoles representing lysosomal glycogen, and were scored 0, 1, 2, or 3 with 0 representing no vacuolization (normal) and 3 representing severe vacuolization. See Table S1 for further details.

PAS-stained sections highlighted the lysosomal glycogen present in the vacuoles observed on H&E section and were scored 0, 1, 2, or 3 with 0 representing no vacuolization (normal), 1-mild vacuolization, 2-moderate, and 3-severe vacuolization.

Histology sections were not evaluated for cytosolic glycogen, due to the variability of glycogen staining in this cellular compartment.

Glycogen concentration

Tissue glycogen concentration was determined by measuring amylo-glucosidase-released glucose from glycogen as described by Canada et al.²⁹ (brain) or Suzuki et al.³⁰ (other tissues).

Glycogen synthase enzymatic activity

Glycogen synthase activity was assessed in tissue homogenates by monitoring the incorporation of glucose from UDP-[U-¹⁴C]glucose into glycogen as previously described.³⁰ Assays were performed in the presence or absence of added glucose-6-P (7.2 mM). The activity

ratio for glycogen synthase was calculated by dividing activity measured in the absence of glucose-6-P by activity measured in the presence of this allosteric activator that induces maximal *Gys1* activity.

Gys1 mRNA expression

RNA was extracted from tissue homogenates (RNeasy Fibrous Tissue Mini Kit, Qiagen). RNA (1 μ g) was reverse transcribed (TaqMan Fast Advanced Cells-to-Ct RT kit, Invitrogen). Quantitative PCR was performed using cDNA corresponding to 80 ng mRNA with Taqman primer-probes targeting *Gys1* and reference genes *Pgk1*, *Ahsa1*, and *Hprt* (ThermoFisher Scientific). *Gys1* expression relative to reference transcripts was determined by the $\Delta\Delta$ Ct method and normalized to vehicle-treated $6^{neo}/6^{neo}$ mice.

GYS1 protein expression

Tissue homogenates were subjected to SDS-PAGE followed by transfer to PVDF membranes that were incubated (BlotBot, Next Advance) with antibodies to GYS1 (1:2,000, Novus NBP3-19957). Secondary antibody was anti-rabbit (1:2,000, Invitrogen A32734). Fluorescence was imaged on a Typhoon 5 (Cytiva) and quantified with ImageQuantTL (Cytiva). GYS1 expression was normalized to total protein (No-Stain Protein Labeling Reagent, Invitrogen).

Statistical analysis

Analysis on all data was done using Prism^R (GraphPad Software). All data are expressed as mean (SD). Analysis of variance (ANOVA) with Tukey's multiple comparison test was used to determine statistical significance between all groups. Unless otherwise noted, percent changes shown in figures indicate comparisons between 6^{neo}/6^{neo} mice treated with vehicle and 6^{neo}/6^{neo} mice treated with ABXC-29.

DATA AND CODE AVAILABILITY

The data that support the key findings of this study are available within the article and supplemental material or upon request from the corresponding author, B.P.

ACKNOWLEDGMENTS

We are grateful to Drew Brown, Diana Jacobs, and Victoria Waldron at Indiana University School of Medicine Histology Core for their excellent work processing and staining histological samples. We are also grateful to Rebecca Rhodes and Vanessa Barcelo-Kreiger for technical support and synthesis of molecules (Aro Biotherapeutics). This work was supported by the National Science Foundation MRI Award Number 2214573 (Typhoon 5 imager). Funding was provided by Aro Biotherapeutics.

AUTHOR CONTRIBUTIONS

Conceptualization, B.A.P., S.G.N., and K.O.; methodology, B.A.P., S.G.N., K.O., R.M., and D.R.; validation, B.A.P.; formal analysis, B.A.P., B.D.H., and S.J.E.; investigation, B.D.H., S.J.E., R.M., and D.R.; resources, Z.D. and S.K.; data curation, B.A.P.; writing—original draft preparation, B.A.P., B.D.H., S.J.E., and S.G.N.; writing—review and editing, B.A.P., B.D.H., S.J.E., S.G.N., and K.O.; visualization, B.A.P., B.D.H., and S.J.E.; supervision, B.A.P.; project administration, B.A.P.; funding acquisition, B.A.P. All authors have read and agreed to the published version of the manuscript.

DECLARATION OF INTERESTS

S.G.N., K.O., Z.D., R.M., D.R., and S.K. are employees of Aro Biotherapeutics.

SUPPLEMENTAL INFORMATION

Supplemental information can be found online at <https://doi.org/10.1016/j.ymthe.2024.11.033>.

REFERENCES

- Heden, T.D., Chow, L.S., Hughey, C.C., and Mashek, D.G. (2022). Regulation and role of glycolysis in skeletal muscle energy metabolism. *Autophagy* 18, 1078–1089. <https://doi.org/10.1080/15486627.2021.1969633>.
- Kohler, L., Puertollano, R., and Raben, N. (2018). Pompe Disease: From Basic Science to Therapy. *Neurotherapeutics* 15, 928–942. <https://doi.org/10.1007/s13311-018-0655-y>.
- van den Hout, H.M.P., Hop, W., van Diggelen, O.P., Smeitink, J.A.M., Smit, G.P.A., Poll-The, B.T.T., Bakker, H.D., Loonen, M.C.B., de Klerk, J.B.C., Reuser, A.J.J., and van der Ploeg, A.T. (2003). The natural course of infantile Pompe's disease: 20 original cases compared with 133 cases from the literature. *Pediatrics* 112, 332–340. <https://doi.org/10.1542/peds.112.2.332>.
- Kishnani, P.S., Corzo, D., Nicolino, M., Byrne, B., Mandel, H., Hwu, W.L., Leslie, N., Levine, J., Spencer, C., McDonald, M., et al. (2007). Recombinant human acid [alpha]-glucosidase: major clinical benefits in infantile-onset Pompe disease. *Neurology* 68, 99–109. <https://doi.org/10.1212/01.wnl.0000251268.41188.04>.
- Chakrapani, A., Vellodi, A., Robinson, P., Jones, S., and Wraith, J.E. (2010). Treatment of infantile Pompe disease with alglucosidase alpha: the UK experience. *J. Inherit. Metab. Dis.* 33, 747–750. <https://doi.org/10.1007/s10545-010-9206-3>.
- Banugaria, S.G., Patel, T.T., and Kishnani, P.S. (2012). Immune modulation in Pompe disease treated with enzyme replacement therapy. *Expert Rev. Clin. Immunol.* 8, 497–499. <https://doi.org/10.1586/eci.12.40>.
- Leon-Astudillo, C., Trivedi, P.D., Sun, R.C., Gentry, M.S., Fuller, D.D., Byrne, B.J., and Corti, M. (2023). Current avenues of gene therapy in Pompe disease. *Curr. Opin. Neurol.* 36, 464–473. <https://doi.org/10.1097/WCO.0000000000001187>.
- Canibano-Fraile, R., Harlaar, L., Dos Santos, C.A., Hoogveen-Westerveld, M., Demmers, J.A.A., Snijders, T., Lijnzaad, P., Verdijk, R.M., van der Beek, N.A.M.E., van Doorn, P.A., et al. (2023). Lysosomal glycogen accumulation in Pompe disease results in disturbed cytoplasmic glycogen metabolism. *J. Inherit. Metab. Dis.* 46, 101–115. <https://doi.org/10.1002/jimd.12560>.
- Taylor, K.M., Meyers, E., Phipps, M., Kishnani, P.S., Cheng, S.H., Scheule, R.K., and Moreland, R.J. (2013). Dysregulation of multiple facets of glycogen metabolism in a murine model of Pompe disease. *PLoS One* 8, e56181. <https://doi.org/10.1371/journal.pone.0056181>.
- Ullman, J.C., Mellem, K.T., Xi, Y., Ramanan, V., Merritt, H., Choy, R., Gujral, T., Young, L.E.A., Blake, K., Tep, S., et al. (2024). Small-molecule inhibition of glycogen synthase 1 for the treatment of Pompe disease and other glycogen storage disorders. *Sci. Transl. Med.* 16, eadf1691. <https://doi.org/10.1126/scitranslmed.adf1691>.
- Douillard-Guilloux, G., Raben, N., Takikita, S., Ferry, A., Vignaud, A., Guillet-Deniau, I., Favier, M., Thurberg, B.L., Roach, P.J., Caillaud, C., and Richard, E. (2010). Restoration of muscle functionality by genetic suppression of glycogen synthesis in a murine model of Pompe disease. *Hum. Mol. Genet.* 19, 684–696. <https://doi.org/10.1093/hmg/ddp535>.
- Weiss, L., Carrer, M., Shmara, A., Cheng, C., Yin, H., Ta, L., Boock, V., Fazeli, Y., Chang, M., Paguio, M., et al. (2024). Skeletal muscle effects of antisense oligonucleotides targeting glycogen synthase 1 in a mouse model of Pompe disease. Preprint at bioRxiv. <https://doi.org/10.1101/2024.02.22.580414>.
- Klein, D., Goldberg, S., Theile, C.S., Dambra, R., Haskell, K., Kuhar, E., Lin, T., Parmar, R., Manoharan, M., Richter, M., et al. (2021). Centyrin ligands for extrahepatic delivery of siRNA. *Mol. Ther.* 29, 2053–2066. <https://doi.org/10.1016/j.ymthe.2021.02.015>.
- Raben, N., Nagaraju, K., Lee, E., Kessler, P., Byrne, B., Lee, L., LaMarca, M., King, C., Ward, J., Sauer, B., and Plotz, P. (1998). Targeted disruption of the acid alpha-glucosidase gene in mice causes an illness with critical features of both infantile and adult human glycogen storage disease type II. *J. Biol. Chem.* 273, 19086–19092.
- Barker, S.J., Thayer, M.B., Kim, C., Tatarakis, D., Simon, M., Dial, R.L., Nilewski, L., Wells, R.C., Zhou, Y., Afetian, M., et al. (2023). Targeting Transferrin Receptor to Transport Antisense Oligonucleotides Across the Blood-Brain Barrier. Preprint at biorxiv. <https://doi.org/10.1101/2023.04.25.538145>.
- Edavettal, S., Cejudo-Martin, P., Dasgupta, B., Yang, D., Buschman, M.D., Domingo, D., Van Kolen, K., Jaiprasat, P., Gordon, R., Schutsky, K., et al. (2022). Enhanced delivery of antibodies across the blood-brain barrier via TEMs with inherent receptor-mediated phagocytosis. *Med* 3, 860–882.e15. <https://doi.org/10.1016/j.medj.2022.09.007>.
- Grimm, H.P., Schumacher, V., Schäfer, M., Imhof-Jung, S., Freskgård, P.O., Brady, K., Hofmann, C., Rüger, P., Schlothauer, T., Göpfert, U., et al. (2023). Delivery of the Brainshuttle amyloid-beta antibody fusion trontinemb to non-human primate brain and projected efficacious dose regimens in humans. *MABS* 15, 2261509. <https://doi.org/10.1080/19420862.2023.2261509>.
- Sonoda, H., Morimoto, H., Yoden, E., Koshimura, Y., Kinoshita, M., Golovina, G., Takagi, H., Yamamoto, R., Minami, K., Mizoguchi, A., et al. (2018). A Blood-Brain-Barrier-Penetrating Anti-human Transferrin Receptor Antibody Fusion Protein for Neuronopathic Mucopolysaccharidosis II. *Mol. Ther.* 26, 1366–1374. <https://doi.org/10.1016/j.ymthe.2018.02.032>.
- Fuller, M., Duplock, S., Turner, C., Davey, P., Brooks, D.A., Hopwood, J.J., and Meikle, P.J. (2012). Mass spectrometric quantification of glycogen to assess primary substrate accumulation in the Pompe mouse. *Anal. Biochem.* 421, 759–763. <https://doi.org/10.1016/j.ab.2011.12.026>.
- Wens, S.C.A., van Gelder, C.M., Kruijshaar, M.E., de Vries, J.M., van der Beek, N.A.M.E., Reuser, A.J.J., van Doorn, P.A., van der Ploeg, A.T., and Brusse, E. (2013). Phenotypic variation within 22 families with Pompe disease. *Orphanet J. Rare Dis.* 8, 182. <https://doi.org/10.1186/1750-1172-8-182>.
- Lee, N.C., Hwu, W.L., Muramatsu, S.I., Falk, D.J., Byrne, B.J., Cheng, C.H., Shih, N.C., Chang, K.L., Tsai, L.K., and Chien, Y.H. (2018). A Neuron-Specific Gene Therapy Relieves Motor Deficits in Pompe Disease Mice. *Mol. Neurobiol.* 55, 5299–5309. <https://doi.org/10.1007/s12035-017-0763-4>.
- Pederson, B.A., Cope, C.R., Schroeder, J.M., Smith, M.W., Irimia, J.M., Thurberg, B.L., DePaoli-Roach, A.A., and Roach, P.J. (2005). Exercise capacity of mice genetically lacking muscle glycogen synthase: in mice, muscle glycogen is not essential

- for exercise. *J. Biol. Chem.* 280, 17260–17265. <https://doi.org/10.1074/jbc.M410448200>.
23. Pederson, B.A., Schroeder, J.M., Parker, G.E., Smith, M.W., DePaoli-Roach, A.A., and Roach, P.J. (2005). Glucose metabolism in mice lacking muscle glycogen synthase. *Diabetes* 54, 3466–3473. <https://doi.org/10.2337/diabetes.54.12.3466>.
24. Pederson, B.A., Chen, H., Schroeder, J.M., Shou, W., DePaoli-Roach, A.A., and Roach, P.J. (2004). Abnormal cardiac development in the absence of heart glycogen. *Mol. Cell. Biol.* 24, 7179–7187. <https://doi.org/10.1128/MCB.24.16.7179-7187.2004>.
25. Xirouchaki, C.E., Mangiafico, S.P., Bate, K., Ruan, Z., Huang, A.M., Tedjosiswoyo, B.W., Lamont, B., Pong, W., Favaloro, J., Blair, A.R., et al. (2016). Impaired glucose metabolism and exercise capacity with muscle-specific glycogen synthase 1 (*gys1*) deletion in adult mice. *Mol. Metab.* 5, 221–232. <https://doi.org/10.1016/j.molmet.2016.01.004>.
26. Gaspar, R.C., Sakuma, I., Nasiri, A., Hubbard, B.T., LaMoia, T.E., Leitner, B.P., Tep, S., Xi, Y., Green, E.M., Ullman, J.C., et al. (2024). Small molecule inhibition of glycogen synthase I reduces muscle glycogen content and improves biomarkers in a mouse model of Pompe disease. *Am. J. Physiol. Endocrinol. Metab.* 327, E524–E532. <https://doi.org/10.1152/ajpendo.00175.2024>.
27. Savage, D.B., Zhai, L., Ravikumar, B., Choi, C.S., Snaar, J.E., McGuire, A.C., Wou, S.E., Medina-Gomez, G., Kim, S., Bock, C.B., et al. (2008). A prevalent variant in PPP1R3A impairs glycogen synthesis and reduces muscle glycogen content in humans and mice. *Plos Med.* 5, e27. <https://doi.org/10.1371/journal.pmed.0050027>.
28. Taksir, T.V., Griffiths, D., Johnson, J., Ryan, S., Shihabuddin, L.S., and Thurberg, B.L. (2007). Optimized preservation of CNS morphology for the identification of glycogen in the Pompe mouse model. *J. Histochem. Cytochem.* 55, 991–998. <https://doi.org/10.1369/jhc.7A7239.2007>.
29. Canada, S.E., Weaver, S.A., Sharpe, S.N., and Pederson, B.A. (2011). Brain glycogen supercompensation in the mouse after recovery from insulin-induced hypoglycemia. *J. Neurosci. Res.* 89, 585–591. <https://doi.org/10.1002/jnr.22579>.
30. Suzuki, Y., Lanner, C., Kim, J.H., Vilardo, P.G., Zhang, H., Yang, J., Cooper, L.D., Steele, M., Kennedy, A., Bock, C.B., et al. (2001). Insulin control of glycogen metabolism in knockout mice lacking the muscle-specific protein phosphatase PP1G/RGL. *Mol. Cell. Biol.* 21, 2683–2694. <https://doi.org/10.1128/MCB.21.8.2683-2694.2001>.